The EUMETSAT Network of Satellite Application Facilities

NWP SAF
Numerical Weather Prediction

Visiting Scientist mission report

Document NWPSAF-EC-VS-020

Version 1.0

21 February 2012

Explicit handling of surface emission for the exploitation of high spectral resolution infrared satellite sounding radiances from IASI over land and sea-ice

B. Ruston[1] and A. McNally[2]

[1] Naval Research Laboratory, Monterey, CA, USA
[2] European Centre for Medium-Range Weather Forecasts, Reading, UK

Met Office

ECMWF

Royal Netherlands Meteorological Institute
Ministry of Transport, Public Works and Water Management

METEO FRANCE
Toujours un temps d'avance

This documentation was developed within the context of the EUMETSAT Satellite Application Facility on Numerical Weather Prediction (NWP SAF), under the Cooperation Agreement dated 1 December, 2006, between EUMETSAT and the Met Office, UK. The partners in the NWP SAF are the Met Office, ECMWF, KNMI and Météo France.

Change record			
Version	Date	Author / changed by	Remarks
1.0	21.2.12	B.Ruston & A.McNally	

Explicit handling of surface emission for the exploitation of high spectral resolution infrared satellite sounding radiances from IASI over land and sea-ice

B. Ruston

Naval Research Laboratory, Monterey, CA

A. McNally

European Centre for Medium-Range Weather Forecasts, Reading, UK

EXECUTIVE SUMMARY

The use of hyperspectral sounding data over land is complicated by increased uncertainty in prior estimates of the surface temperature and emissivity provided by the NWP model. These larger errors are more difficult to characterise in the assimilation system and also limit our ability to successfully detect cloud contamination in the observed radiances. As a result, a common practice at operational NWP centres is to remove any radiance data with appreciable signal from the surface over land and ice. This leaves large expanses of the globe systematically unobserved by infrared radiances (e.g. Canada and northern Eurasia). This study focuses on the use of IASI radiance data over land and ice surfaces, specifically estimating an effective radiative skin temperature (that includes emissivity) during the analysis, simultaneously with other atmospheric variables. The accuracy of prior estimates of skin temperature (from the NWP model) is investigated and the reduction of error that can be achieved when IASI radiances are used is quantified with simulations. The simulations suggest that the IASI channels convey a substantial amount of information on the surface and that errors in the estimation of skin temperature are relatively decoupled from those of atmospheric variables. This is important as it means that even over complex terrain when prior skin temperature errors are large, these can be handled successfully with minimal damage to the analysis of atmospheric levels above. These findings have been tested in a real assimilation context using IASI radiances in the ECMWF 4D-Var. The main developments required were a modified characterisation of background error for skin temperature (that reflected uncertainties over land) and a new method to detect cloud contamination in IASI spectra over land (that did not rely on a highly accurate prior estimate of the skin temperature). For the latter, AVHRR imagery collocated inside the IASI pixel has been used to indicate scene heterogeneity and used as a proxy for the presence of cloud. Results from the assimilation experiments suggest that a substantial amount of IASI radiance data can be successfully used over land surfaces and these data lead to some modest improvements in the analysis and forecasting of the lower troposphere.

1. Introduction

This first task in this study is to quantify the accuracy of prior estimates of skin temperature over land from the NWP model. Very few independent observations of radiative skin temperature exist, so departures of observed satellite radiance from values computed from the NWP model (with skin temperature as input) in the most transparent window channels are used as a proxy. Statistics of these departures (carefully screened to remove signals due to cloud) are presented and provide indirect information on the typical range of skin temperature errors and their geographic variation with season.

Having quantified the accuracy of prior information on skin temperature over land, the information brought by radiance measurements from IASI is then studied. In this section we attempt to simulate the performance of these radiance observations in a full 4D-Var system with an offline linear optimal estimator. With this results are presented that show how accurately skin temperature can be estimated using the operational ECMWF IASI channels set, but also how errors in the analysis of skin temperature are correlated with the errors in the atmosphere above.

Using this offline optimal estimator we further investigate the sensitivity information to atmospheric state - both due to the variation of background error covariances provided by the ECMWF Ensemble of Data Assimilations (EDA) and the inherent nonlinearity of the radiance jacobians. The implications of wrongly specifying of background errors for skin temperature are also tested.

Based upon experience from the simulations, real data assimilation experiments using IASI radiances over land are performed. The development of a strategy for cloud detection using collocated AVHRR imager products is described as well as the tuning of background errors for skin temperature over land. The impact of assimilating the additional IASI observations over land upon the quality of the ECMWF analysis and forecasting system is documented.

Finally the study is summarised and some perspectives for future studies are presented.

2. Errors in prior estimates of skin temperature from the NWP model

In the current ECMWF data assimilation system the surface skin temperature is represented by a single analysis variable defined at each observed radiance location. The skin temperature is decoupled from other atmospheric variables in the background error covariance and has no constraints imposed upon spatial consistency. During the analysis the background value of the skin temperature (provided by the NWP model) is evolved and adjusted to fit the observed radiances during the minimisations. However, at the end of the analysis the evolved value is essentially discarded and not passed on to the next assimilation window. Thus the surface skin temperature is primarily intended to act as a sink variable in the ECMWF analysis, to absorb surface forcing signals from the radiances (but also from undetected residual cloud) and protect the analysis from any potential aliasing of these into erroneous atmospheric increments. Over land a background error of 5K is currently assumed for the surface skin temperature variable. This value should reflect the combined uncertainty in the value of skin temperature provided by the NWP model and un-modelled variations in land surface emissivity (currently specified as a constant 0.98).

No independent direct measurements of land surface skin temperature or emissivity exist from which the validity of the assumed background error (5K) can be tested. The first-guess departures (i.e. observed minus background) in infrared window channels should provide some guidance, but of course these have limitations. Firstly, statistics of the departures include an additional component due to observation and radiative transfer error. Secondly, even the cleanest infrared window channels are subject to some attenuation in the atmosphere (by water vapour) and thus have a reduced sensitivity to errors in the surface emission. Departures statistics have been studied in two infrared window channels: channel 1191 (10.61 microns) in the long-wave, and channel 7785 (3.82 microns) in the short-wave, accumulated over two periods from 15Dec2010 - 15Feb2011 (DJF) and from 01Jul2011 - 01Sep2011 (JAS). The following quality control (QC) steps have been applied: Firstly, to avoid signals due to solar contamination, the shortwave channel 7885 is only evaluated during the night which is defined as when the solar zenith angle is greater than 105 degrees. Secondly, to avoid signals from cloud contamination, data are only accepted if collocated AVHRR pixels within the IASI footprint have a standard deviation less than 1 W/m^2, and a mean radiance greater than 55 W/ m^2. The latter check is aimed at removing IASI footprints covered by homogeneous cold cloud (that may still have a very low pixel standard deviation).

Maps of the mean and standard deviation of first guess departure in the two channels averaged over the two periods are shown in figures 1 to 4. Also shown in these figures are scatter plots where the statistics have been displayed as a function of Leaf Area Index (LAI). This is defined as one-half the total green leaf area per unit ground surface area and the derivation in the context of the ECMWF DA system is described by Bousetta in ECMWF Technical Memoranda 640 (2011). The LAI is considered an important parameter because the more difficult terrain to model, i.e. mountainous and desert, are generally barren terrain and can be readily identified using this parameter which has values ranging from 0 – 6.

In the more atmospherically transparent channel 7885 at night time, the DJF mean shows a more consistent negative first-guess departure which in the summer is only seen for the more barren terrain. These mean departure errors point towards the model underestimating the minima reached over the land surfaces particularly in the Northern Hemispheric winter. The mean standard deviation for each integer range of LAI is shown by the gray boxes with the total number of points in the range shown inside the box. This shows that a typical night time standard deviation for DJF is approximately 2K and slightly lower for JAS 1.5K. For both the majority of values are between 0.5 and 3.5K. For the daytime, the 1191 channel is used, but this can have an atmospheric transmittances in the tropics and mid-latitudes between 0.4 and 0.6, and is thus less sensitive to the surface emission error. The mean departures of the daytime for DJF and JAS are centred generally around 0K. The standard deviations of these departures is much more tightly grouped in the DJF case than the NH summer months of JAS. The standard deviations lie generally about 2K, but the spread of standard deviations is broader than seen in the night time for channel 7885, with the DJF range between 0.5 - 4K and the JAS months having a broad range between 0.5 - 4.5K. What is noticeable for the JAS months is that many of the higher standard deviations such as in Northern Eurasia and the southern Sahara and Arabian peninsula often tend towards a 0K mean values, while the north eastern Sahara and northern Arabian peninsula and the region to the East of the Caspian Sea which has higher mean departures show a more stable standard deviation.

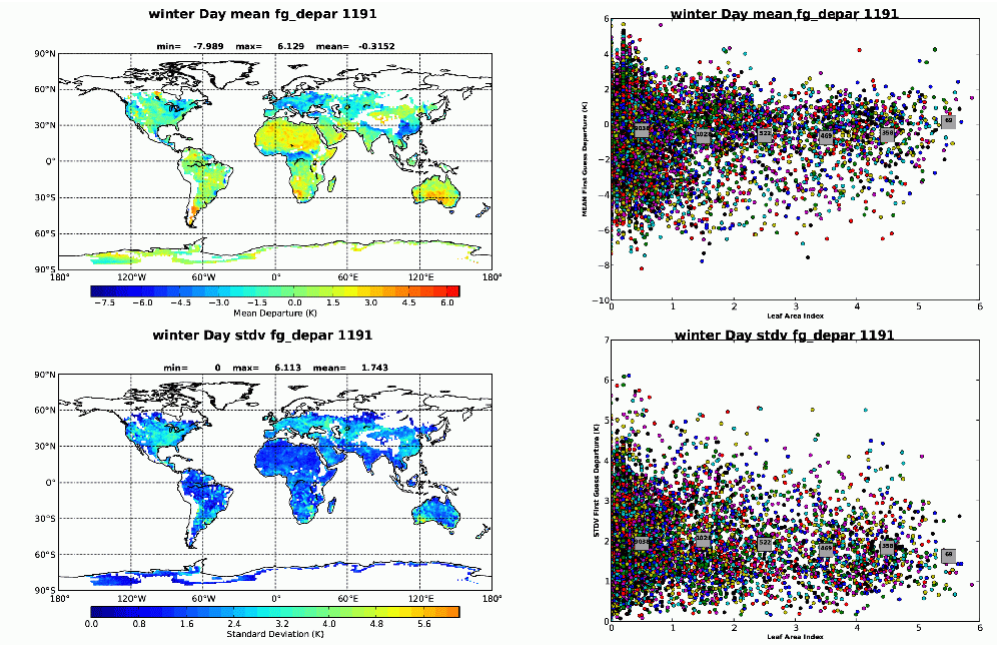

Figure 1 Mean and standard deviation of first-guess departures in channel 1191, and scatter plots of the mean and stdv of first-guess departures against Leaf Area Index (LAI) for 15Dec2010-15Feb2011 (DJF) daytime.

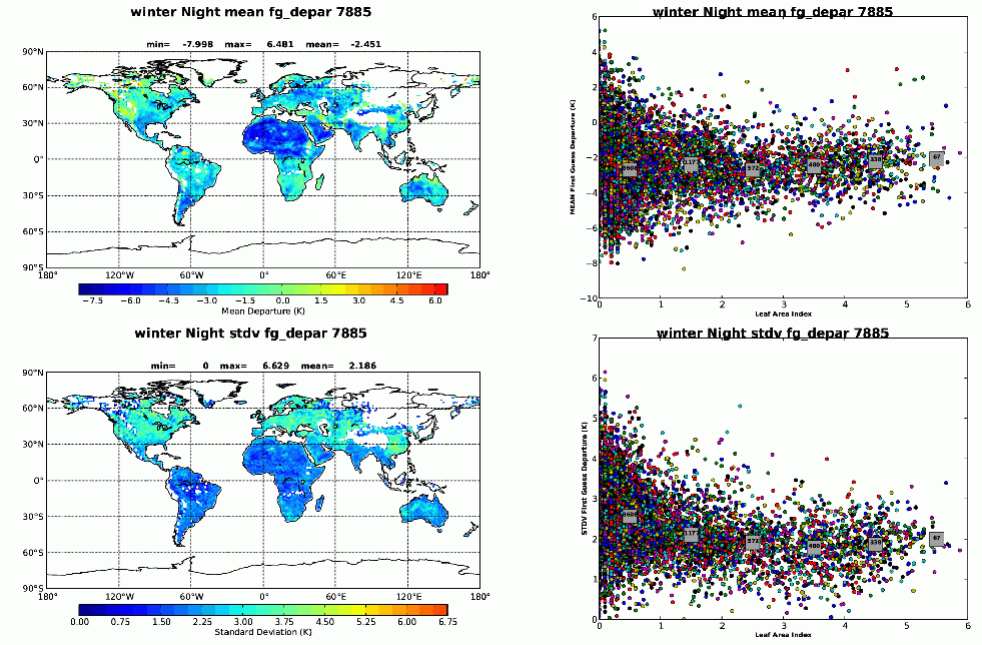

Figure 2 Mean and standard deviation of first-guess departures in channel 7885, and scatter plots of the mean and stdv of first-guess departures against Leaf Area Index (LAI) for 15Dec2010-15Feb2011 (DJF) daytime.

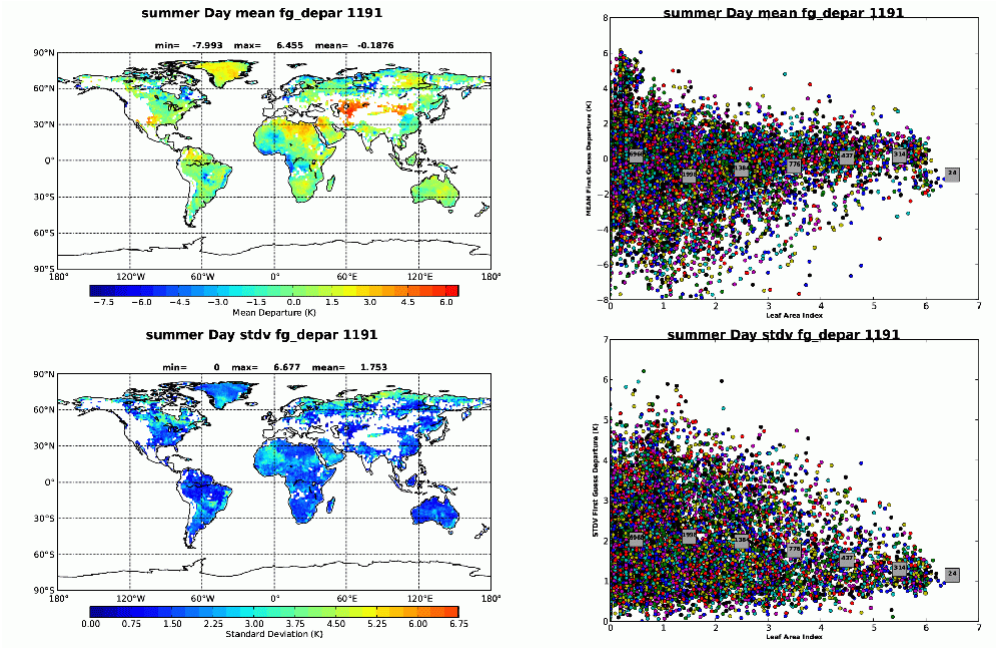

Figure 3 Mean and standard deviation of first-guess departures in channel 1191, and scatter plots of the mean and stdv of first-guess departures against Leaf Area Index (LAI) for 01Jul2011-01Sep2011 (JAS)

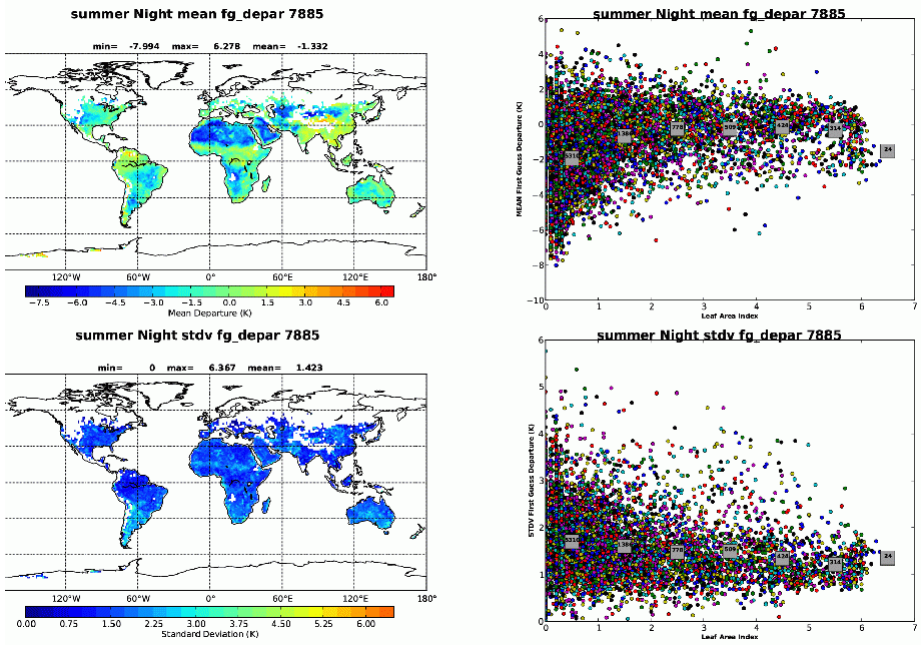

Figure 4 Mean and standard deviation of first-guess departures in channel7885, and scatter plots of the mean and stdv of first-guess departures against Leaf Area Index (LAI) for 01Jul2011-01Sep2011 (JAS)

On the basis of these statistics we may conclude that specifying the background error for the effective surface skin temperature to 5K is likely to be an overestimate and that values in the range 2K to 3K would be more appropriate. However, it is important to point out that these values are only applicable to the assimilation of this population of IASI data (i.e. data passing the QC outline above). They cannot be applied to IASI data in other circumstances, nor can they be applied to other satellite data that may sample a different diurnal phase of the model's surface temperature scheme that has different error characteristics.

3. Skin temperature estimation in the analysis

In this part of the study we attempt to simulate what happens when observed radiance spectra from IASI are assimilated in the ECMWF 4D-Var. For this we use a simple analysis of a linear 1D optimal estimation and its error covariance. We quantify to what extent the skin temperature can be estimated independently of the other analysis variables by examining inter-level correlations in the analysis error covariance. The impact of mis-specification of the background errors for skin temperature is then investigated by constructing sub-optimal analysis error covariances. Finally, the relevance of these findings is assessed by comparing how well surface temperature increments in the full 4D-Var are reproduced by this simple linear optimal estimator.

3.1 The optimal case

The maximum likelihood solution, which is the fundamental basis of the 4D-Var analysis scheme, can be represented in 1 dimension by the expression:

$$X^{OPT} = X_B + W [Y_{OBS} - Y(X_B)]$$

Where the optimal weights applied to the radiance departures are given by:

$$W = (HB)^T [HBH^T + (O + F)]^{-1}$$

Here the matrix B is the background error covariance, the matrix (O+F) is the combined observation and forward model error and H is the matrix of radiance jacobians for the IASI channels to be assimilated. The optimal error in the analysis is given by the expression:

$$S^{OPT} = B - W B H$$

It can be seen that, in the optimal case, the diagonals of the analysis error covariance are always less than the corresponding values from the background error covariance - indicating (as expected) that the observed radiances have reduced the uncertainty in our knowledge of the atmospheric state (and surface parameters). The diagonals of S^{OPT} and B are shown in figure 5 as a function of atmospheric pressure. The dots indicate analysis error values for the surface skin temperature. In the creation of these error estimates the observation error corresponds to that assumed in the operational system at ECMWF which is a step-function for spectral bands (minimum 0.4K for tropospheric temperature sounding channels, maximum 2.0K for window channels). Jacobian matrices were computed for U.S. standard atmospheres (N.Polar, N Mid Lat and Tropical) using

RTTOV-9 as described in Matricardi et al. 2003 and Matricardi 2009 for the 366 channels processed operationally at ECMWF. The background error covariances for atmospheric variables are taken from averages from the operational ECMWF hybrid EDA 4D-Var system over 30-degree latitude bands. For the moisture variable only the correlation structures are taken from the averages, while the standard deviation of the specific humidity is computed from point values representative to each region using the humidity transform and resulting error estimation from version 37R3 of the ECMWF assimilation system (Gustafsson et. al, 2011). For the surface skin temperature an error of 2.5K has been assumed on the basis of the results from the previous section.

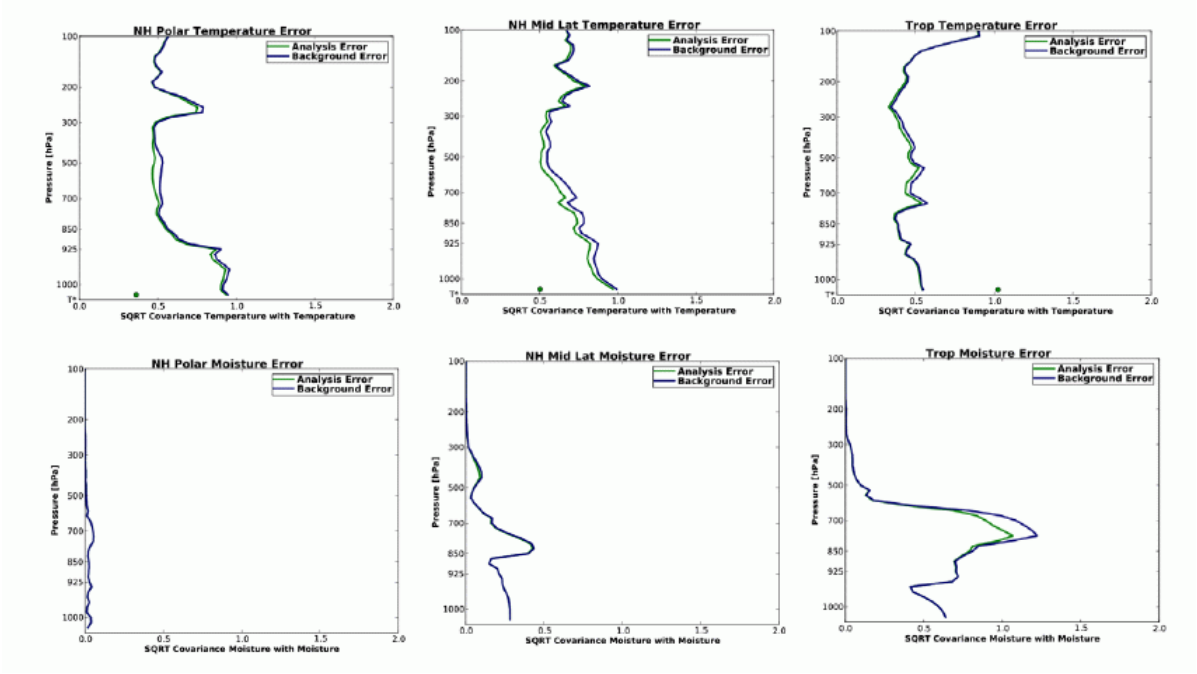

Figure 5 Diagonals of the analysis and background error covariances for optimal estimation of temperature (upper panels) and humidity (lower panels) evaluated in three standard atmosphere (left N.Polar, centre NH Mid-lat and right Tropics). Skin temperature analysis errors are shown by the dots on the x-axis of the upper plots.

Under these conditions it can be seen in figure 5 that the improvements over the background estimate of atmospheric temperature and humidity are small. This is a result of two factors: firstly the background is rather accurate throughout most of the troposphere with errors in the region of 0.5K in temperature and equivalent to just a few percent in humidity. Secondly these small errors are not strongly coupled in the vertical (i.e. the vertical modes of error are very sharp) as seen later in the correlation structures inferred from figure 6. Even with many hundreds of channels the information provided by nadir sounding instruments is still very limited to correct sharp vertical structures.

In contrast to the atmosphere, it can be seen that improvements over the background for surface skin temperature can be significant. The initial uncertainty of 2.5K is reduced to less than 0.5K in dry conditions, and even in the tropics when large water vapour concentrations partially obscure the surface, an accuracy of 1K is still maintained. This shows that even the standard 366 IASI channels

(that were designed as a general purpose NWP set) convey a significant amount of information from which the surface skin temperature can be estimated.

When we examine the correlation structure of the background and analysis error covariance matrices in figure 6 we see that in the atmosphere, the reduction in the magnitude of error (diagonals) from assimilating the radiance information is associated with a change in the degree of inter-level correlation. In the background, temperature errors are rather localised in the vertical, being correlated over just a few adjacent levels. The radiance assimilation produces an analysis with similarly correlated adjacent levels, but leads to slightly stronger anti-correlations between levels at greater distances.

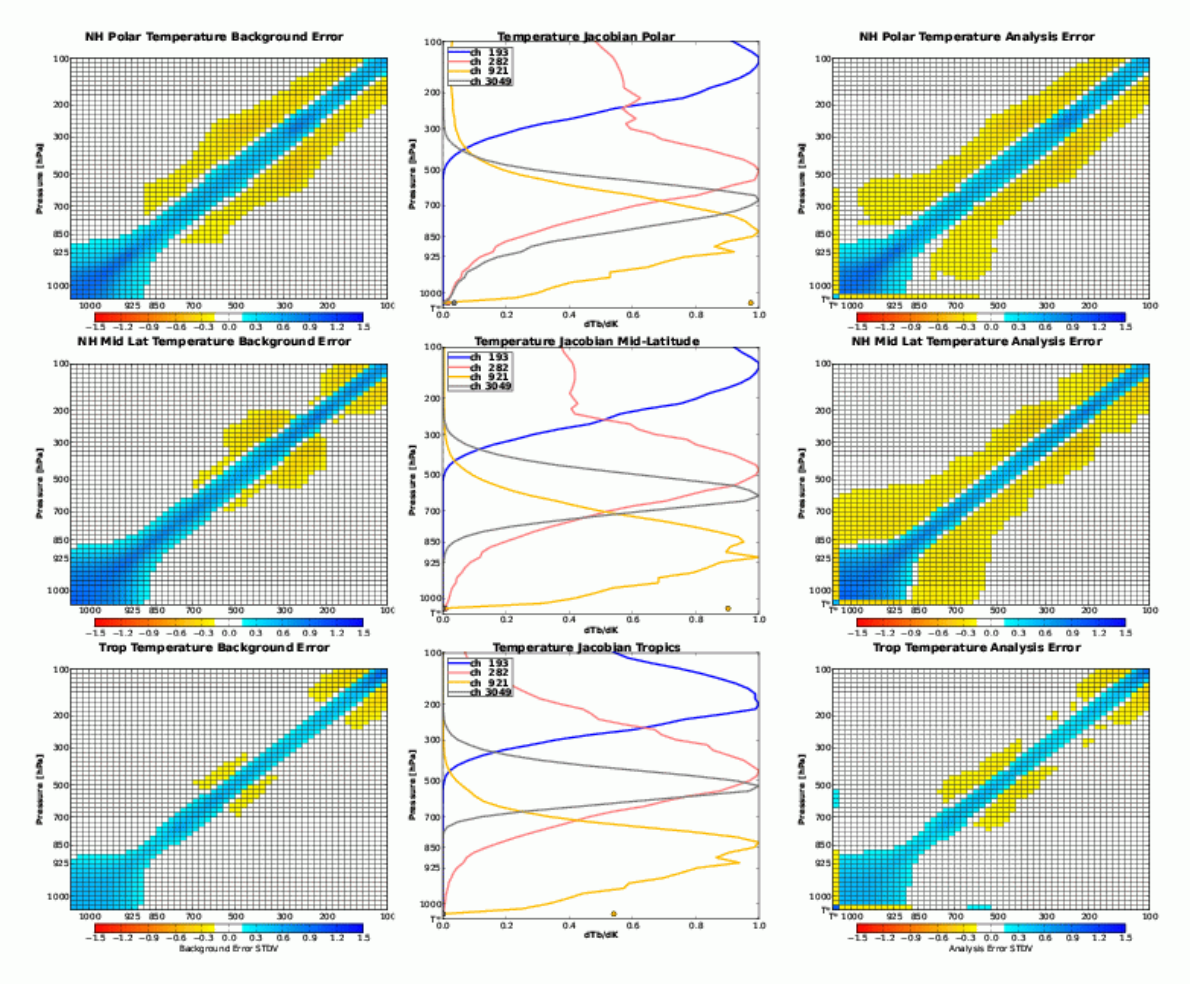

Figure 6 Corrleations of the analysis and background error covariances for optimal estimation of temperature evaluated in three standard atmosphere uppert N.Polar, centre NH Mid-lat and lowerTropics). The centre column panels show jacobians in 4 typical sounding channels.

For the surface skin temperature, background errors are completely uncorrelated with the levels above (by construction) and we might expect the analysis of channels that are sensitive to both the atmosphere and the skin temperature to introduce correlations between these variables. However,

it can be seen in figure 6 that these standard deviations of temperature remain rather small (< 0.2K) and are insignificant above 700hPa. A very important conclusion from this is that the atmospheric parameters (certainly above 700hPa) can be estimated independently from the surface skin temperature (and vice–versa) such that we should be able to successfully assimilate IASI radiances over land as long as the surface skin temperature is estimated simultaneously.

3.2 The sub-optimal case

Of course the conclusion above only holds as long as the assumptions in our simple linear analysis are valid. We are fairly confident that for the population of quality controlled clear-sky cases a background error of 2.5K is quite reasonable. However, it makes sense to quantify how errors in this assumption would adversely damage the estimation of skin temperature and, more importantly, compromise the quality of the atmospheric analysis in the levels above.

To estimate this impact we will follow a strategy used by McNally (2000). In the optimal case the maximum likelihood weights in the linear estimator should be

$$W = (HB)^T [HBH^T + (O + F)]^{-1}$$

But we deliberately mis-specify the background error for surface skin temperature in the covariance B^{SUB} and form the incorrect weights

$$W^{SUB} = (HB^{SUB})^T [HB^{SUB}H^T + (O + F)]^{-1}$$

In this case it can be shown that the error in the sub-optimal analysis estimate is given by the expression:

$$S^{SUB} = (I - W^{SUB} H) B (I- W^{SUB} H)^T + W^{SUB} (O+F) W^{SUB\ T}$$

We can thus quantify the impact of incorrect assumptions about the accuracy of the prior information about surface skin temperature. This is done in figure 7 where we assume a skin temperature error of 2.5K, but simulate cases when the true skin temperature error varies by up to a factor of 5 (larger and smaller). It can be seen that when the assumed skin temperature error is an overestimate of the truth there is very little degradation of the skin temperature estimate or the atmospheric analysis above. When the assumed error is significantly less than the true value, the skin temperature error degrades significantly and the atmospheric analysis errors can degrade to be worse than the background in the lower tropospheric levels.

This asymmetry is intuitively reasonable. When the skin temperature error is overestimated radiance signals pertaining to the atmosphere may be wrongly dumped in to adjustments of the skin temperature variable. However, signals from the atmosphere are generally small, so this does not lead to significant degradation of either the atmospheric or skin temperature analysis. When the skin temperature errors are significantly underestimated, radiance signals pertaining to the surface can be wrongly aliased into erroneous adjustments of the atmosphere. As the magnitude of the surface signals are larger, this aliasing can lead to a serious degradation of the atmospheric analysis.

Thus the conclusion from this simulation is that – while every attempt should be made to correctly specify the background skin temperature error – if significant uncertainty exists it is better to overestimate the errors and avoid underestimation.

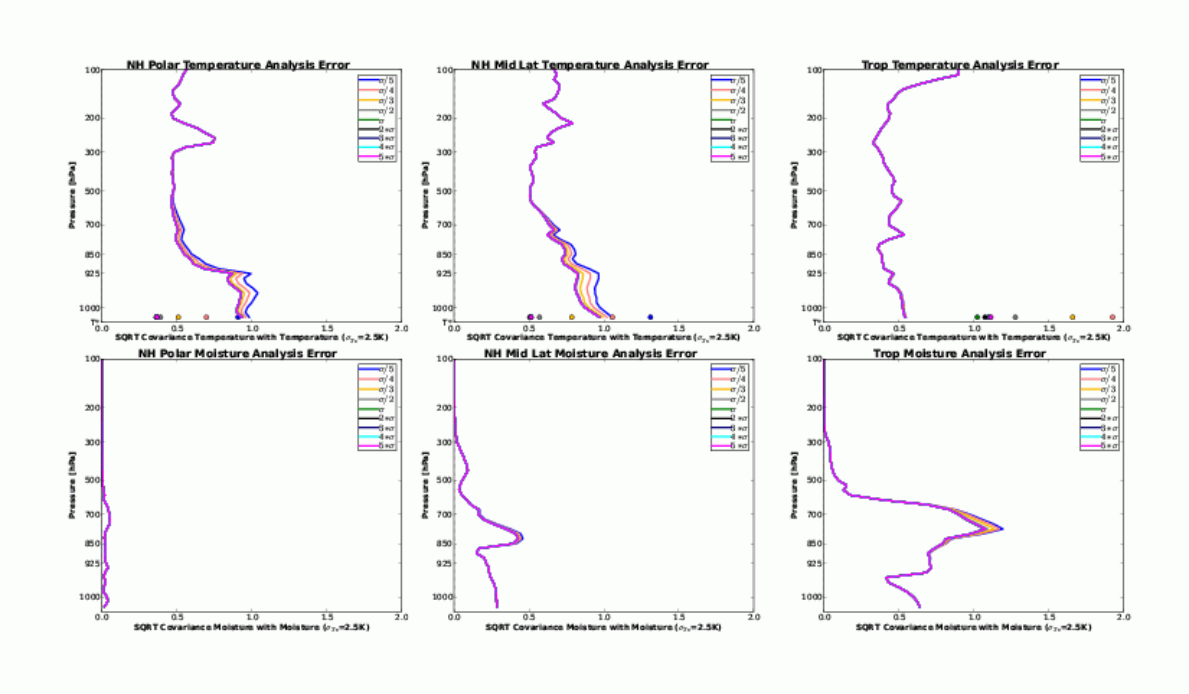

Figure 7 The diagonal of the sub-optimal analysis error where different specification of skin temperature errors are assumed

3.3 Offline simulation of skin temperature adjustments in the full 4D-Var

The ECMWF 4D-Var analysis has been run in test mode where IASI radiances are assimilated over land (operationally spectra measured over are blacklisted and excluded from the analysis). The first stage in the analysis supplies time and space interpolated background fields of the atmospheric and surface parameters to the RTTOV radiative transfer operator and spectra $Y(X_B)$ are computed at every observation location. These are compared to the observed IASI spectra Y_{OBS} and the radiance departure vectors $[Y_{OBS} - Y(X_B)]$ are stored. The radiance departures are the initial basis of the iterative adjustment process in the full 4D-Var, in which increments (changes) are made to the atmospheric and surface variables to maximise the fit to the radiance observations while respecting the fit of the analysis to the background information according to the background error covariance. However, in the full 4D-Var system there are significant additional constraints imposed upon the adjustment process including considerations of balance, time consistency with the forecast model equations and of course the fit to other observations.

A selection of these initial radiance departure vectors have been extracted and supplied to the 1D linear estimator described previously to answer the question to what extent can the adjustments of the full 4D-Var scheme be mimicked offline by the simple 1D estimator. In the latter the weights applied to the radiance departure vector only optimise the fit to the measured radiances and the

background (according to its error covariance) and no account is taken of the additional constraints of the full 4D-Var system. To improve the realism of the simple 1D estimator, weights have been

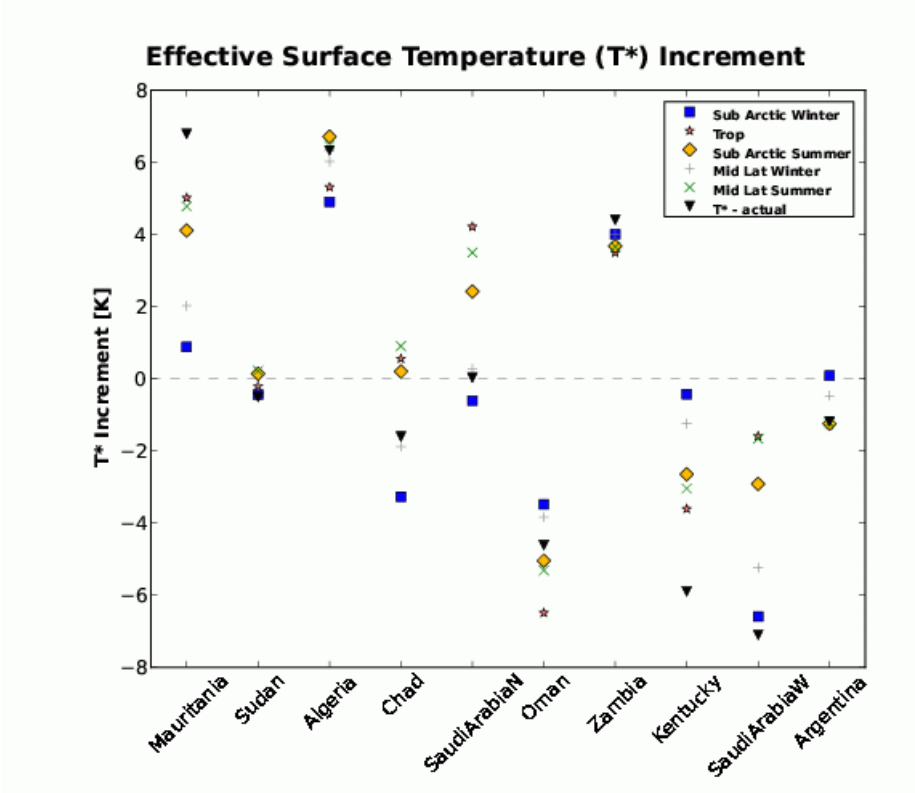

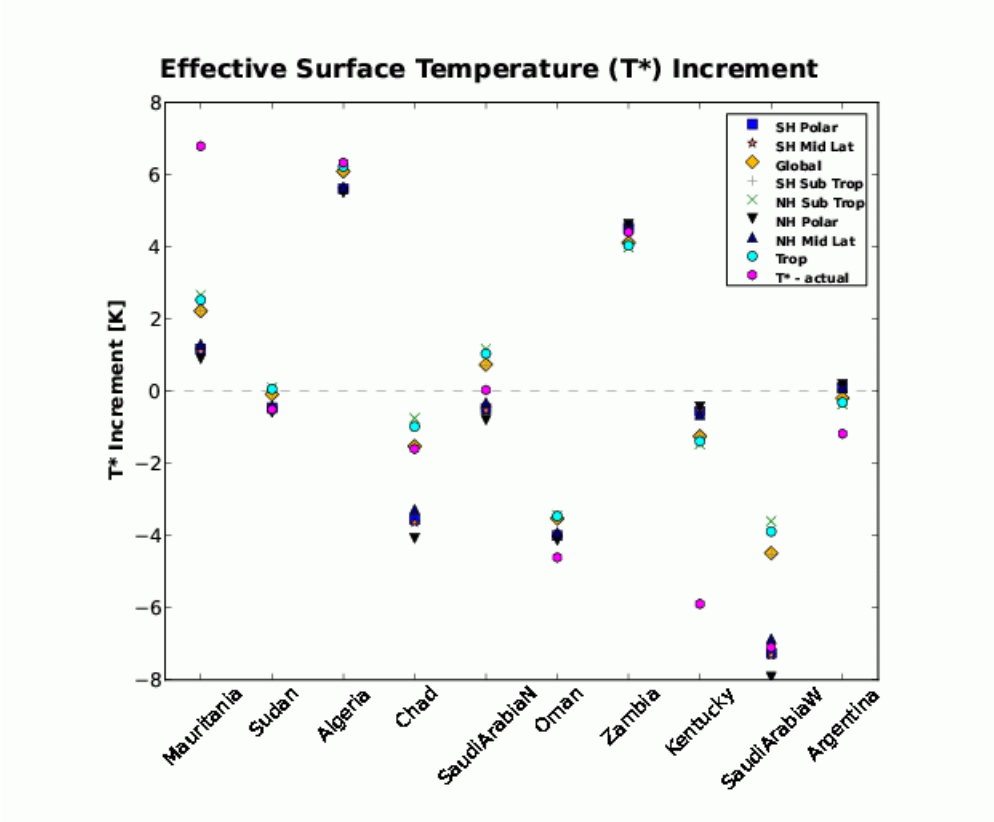

Figure 8 Offline simulations of the skin temperature adjustment in the full 4D-Var using a variety of jacobians in different atmospheres (upper panel) and a variety assumptions of background errors for the atmosphere.

computed taking in to account two sources of variability that are implicitly accounted for in the full 4D-Var. Firstly, different weights are generated using geographically varying estimates of the atmospheric background error covariance matrix B. Secondly, the weights have been generated using state dependent jacobians from a selection of US standard.

Skin temperature adjustments for the variety of cases that have been examined are shown in figure 8. It can be seen that the offline simple system compares qualitatively rather well with the skin temperature adjustments from the full 4D-Var – reproducing both large warming and cooling of the skin temperature up to several degrees. The results further show that the sensitivity to jacobian specification is stronger than that to the characterisation of the atmospheric background error covariance.

We may conclude from this comparison that the important additional constraints present in the full 4D-Var have only a weak indirect effect (via the atmosphere) upon the surface skin temperature, which to a large extent is adjusted in a simple 1D sense. This gives us some confidence that the indications from the previous simulations are valid to the full scheme.

4. Real data assimilation experiments with IASI radiances over land

Experiments to test the impact of assimilating IASI radiance data over land have been run. The experimental period covers 3 months from the 1 June to 29 August 2011.

4.1 The baseline operational system

The baseline system for these tests is version 37R3 of the ECMWF operational analysis and forecast system, run a reduced spatial resolution of T511 (typical grid spacing 40Km). All observations are assimilated (satellite and conventional) including IASI radiances from the 366 channel set. The surface skin temperature sink variable, T*, is active for all radiance observations. Over oceans the background error for this variable is set to 1K , and over land and ice surfaces the background error is set to 5K. Mixed terrain model grid boxes have a value interpolated according to the fraction of land and sea. While the skin temperature variable is active over land, in the baseline operational system IASI radiances are not assimilated over land (although some channels from AMSUA are active over land). The 4D-Var analysis is incremental, involving three outer loops. The background estimate of T* comes from the NWP model and is updated during each minimisation. The updated value of T* is then passed on to successive outer loops (see annex A for a note on this).

The cloud screening of IASI data seeks to identify a subset of clear channels in a potentially cloudy field of view using the algorithm described in McNally and Watts (2003). Channels with appreciable cloud contamination are rejected. A recent addition is the assimilation of all IASI channels when a scene is determined to be completely overcast with homogeneous cloud. At these locations the

cloud top pressure is estimated and adjusted simultaneously with other variables during the 4D-Var (McNally 2009).

IASI radiance observation errors range between values of 0.4K for the long-wave temperature sounding channels in the troposphere up to values of 2.0K for window channels with a strong sensitivity to the surface. Systematic errors in the IASI radiances are removed by an adaptive variational bias correction scheme in common with all other satellite radiances.

4.2 The experimental system with IASI data over land

The experimental system is identical to the baseline except it aims to make additional use of IASI radiances over land. However, a significant modification was required in the handling of clouds. The operational cloud detection scheme (to find clear channels) and the cloud estimation scheme (to identify overcast scenes) both rely on an accurate estimate of the surface emission. Thus the performance of these schemes may be degraded over land surfaces when skin temperature errors can be significantly larger than those for ocean. For this reason the assimilation of overcast data over land is not attempted at all and the identification of clear channels over land is performed with a hybrid approach.

Thresholds for the mean and standard deviation of collocated AVHRR imager data inside the IASI field of view are applied to identify completely clear locations as was done in section 2. If these checks are passed all channels are retained for assimilation at that location. If these AVHRR checks fail, all channels sensitive to the mid-lower troposphere are rejected, but channels peaking higher in the atmosphere (with no sensitivity to surface emission) are checked using the operational cloud detection algorithm. Any channels determined cloud free by this check are also retained for assimilation (note the lowest peaking channel considered in this way is IASI 232 peaking around 150hPa).

The only other modifications compared to the baseline system is that the background error for skin temperature over land (at IASI locations) is reduced to 2.5K (based on the window channel statistics of section 2), coastal points with land fractions less than 95% are excluded and locations where the radiance departures in the long-wave window channel 1191 either exceed 6.5K or are below -8.5K. The latter check is intended as a safety measure to ensure that instances where the land surface skin temperature is grossly in error are not assimilated and corresponds to roughly 3 times the assumed background error.

4.3 Changes to the analysis when IASI is used over land

A typical example of the additional data coverage from using IASI over land is shown in figure 9 for a window channel 921 and channel 232 peaking around 150hPa. It can be seen that with the current (rather conservative) QC thresholds applied to the AVHRR and window channel departures, most of the extra observations in the lower tropospheric channels (e.g. 921) are located in Africa, South America and Australia. It is perhaps surprising that the data coverage of channel 232 is also rather limited as the AVHRR cloud check is not applied, but the operational cloud screening algorithm is

used. We can only conclude that the significant sensitivity of this channel to levels (and therefore cloud contamination) below its peak results in these rejections.

The observed minus background radiance departures for these two channels are also shown in figure 9. For the window channel 921 values are, as expected, considerably larger than data

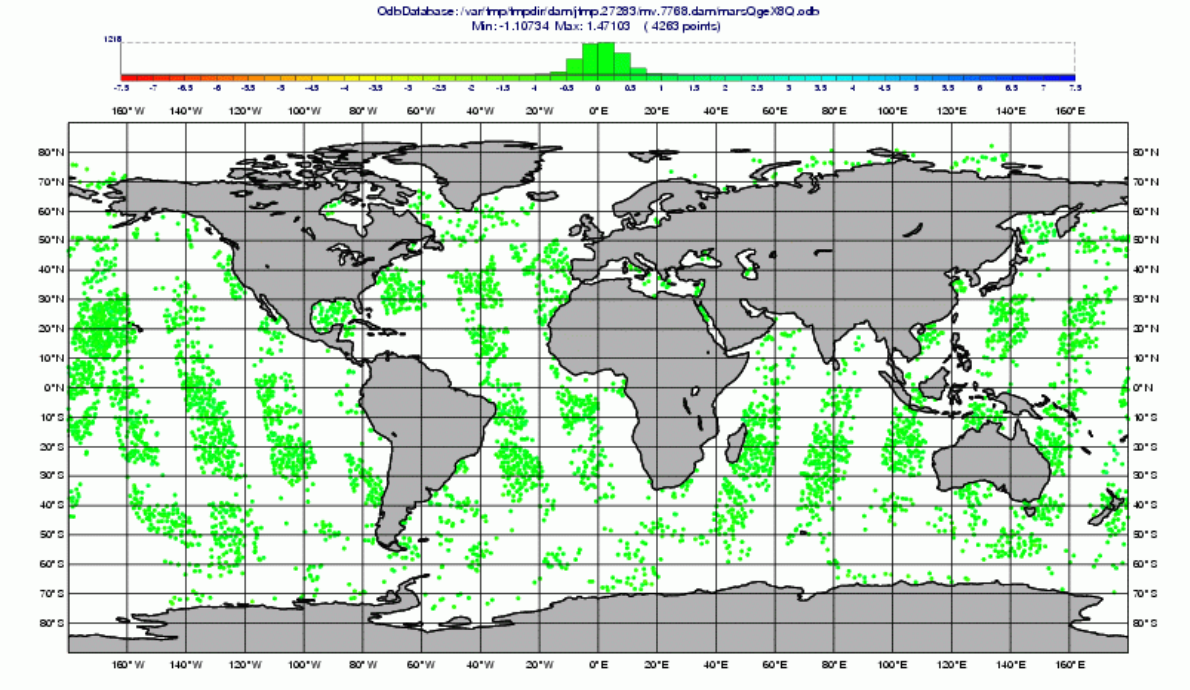

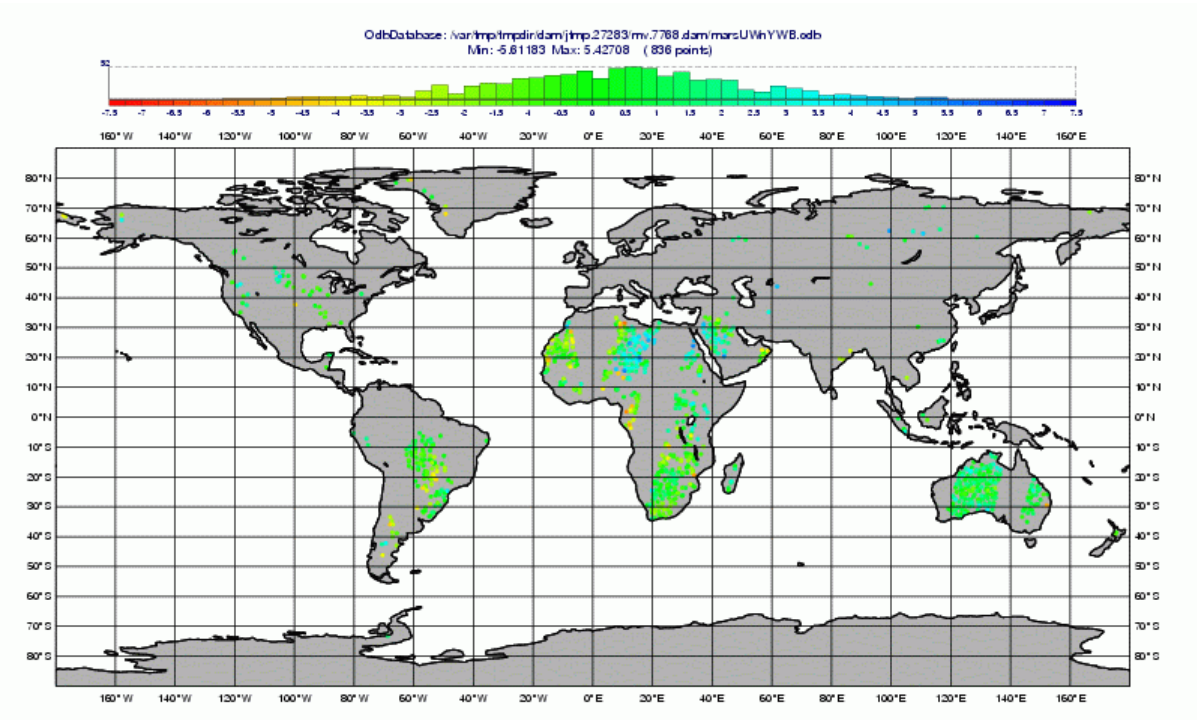

Figure 9 Typical data coverage of IASI channel 921 passing the QC checks and being assimilated for the 00z 12hr window on 2011-06-01 over sea (upper panel) and over land (lower panel). The marker colour and histogram indicates the size of the radiance departure in K.

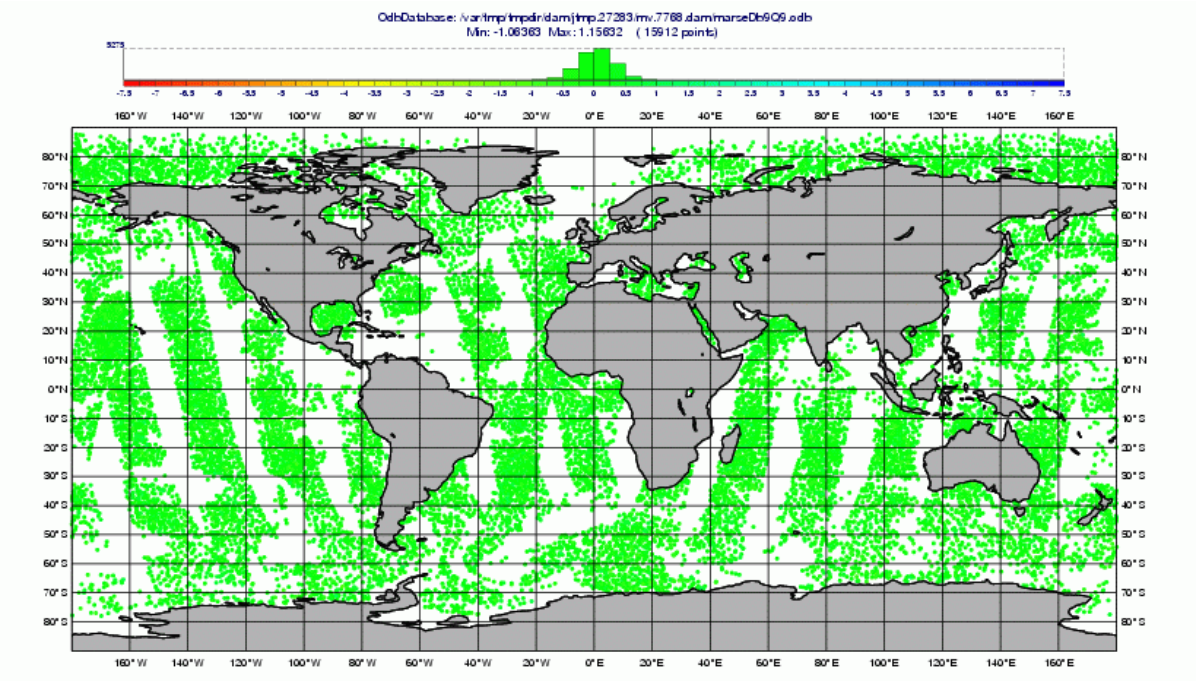

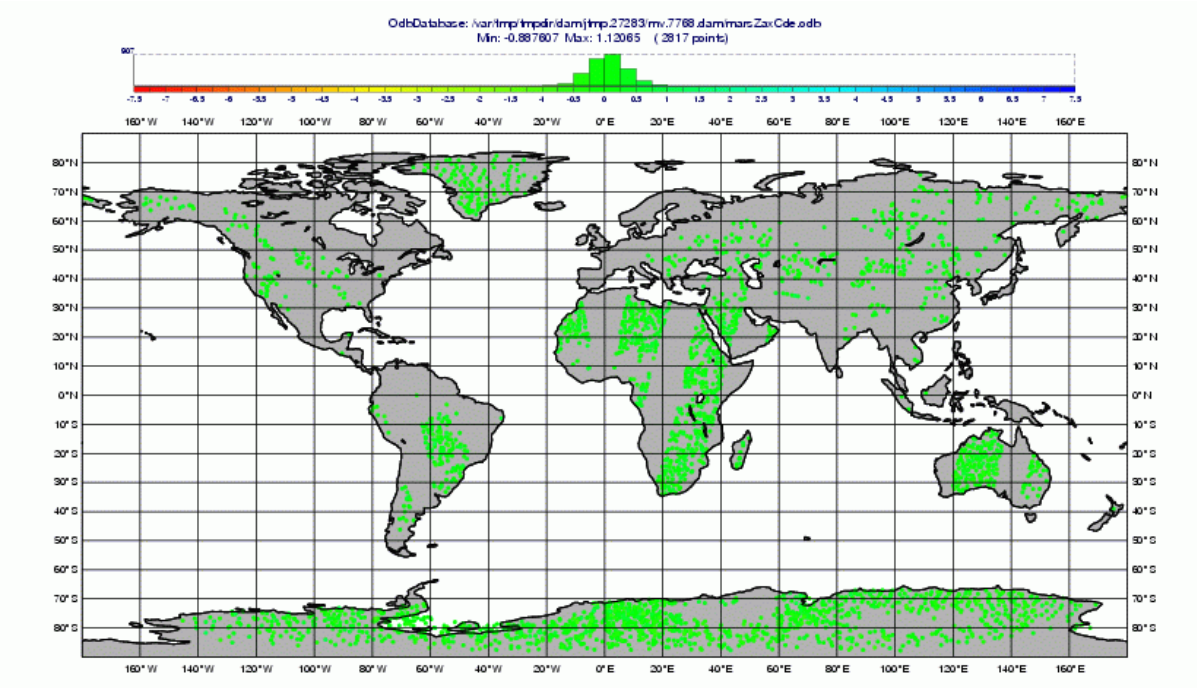

Figure 9 Typical data coverage of IASI channel2321 passing the QC checks and being assimilated for the 00z 12hr window on 2011-06-01 over sea (upper panel) and over land (lower panel). The marker colour and histogram indicates the size of the radiance departure in K.

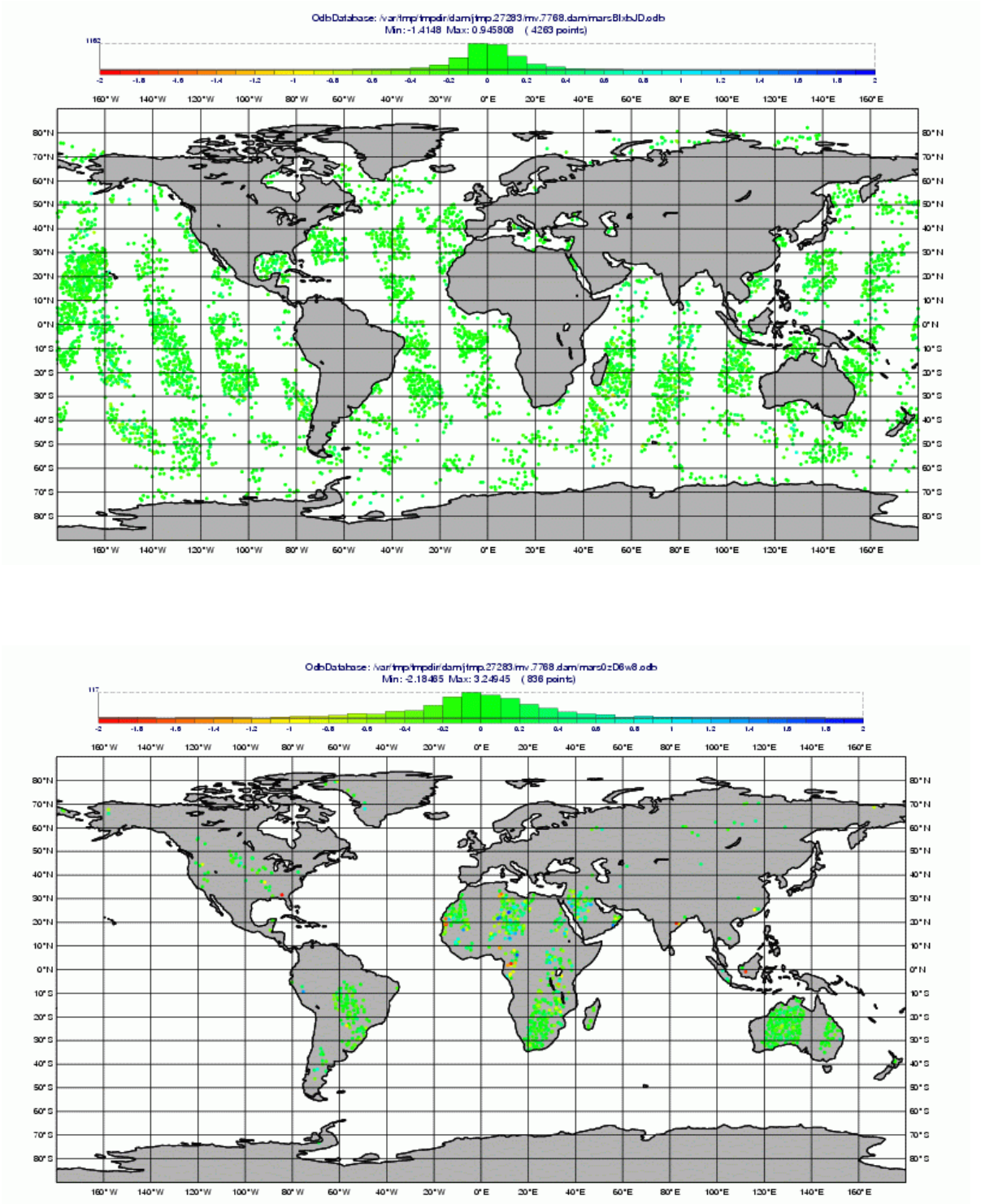

Figure 10 Typical data coverage of IASI channel 921 passing the QC checks and being assimilated for the 00z 12hr window on 2011-06-01 over sea (upper panel) and over land (lower panel). The marker colour and histogram indicates the size of the skin temperature adjustment at the IASI locations.

measured in the same channel over sea. In the higher peaking channel 232 the radiance departures over land are very similar to those over sea and this gives us confidence that the data selection and cloud checking applied to these higher sounding channels are working well.

The magnitude of the skin temperature adjustment from the background value at IASI locations is shown in figure 10 (only for locations over land when channel 921 is assimilated). The size of the adjustments appears reasonable – typically less than 3K and is consistent with the magnitude of the radiance departures of the accepted data. For comparison the smaller adjustments of the skin temperature over sea locations is also shown in figure 10.

In the atmospheric analysis above the land surface additional temperature and humidity increments due to the assimilation of IASI are generally found to be rather small. Excess temperature increments (defined as the RMS increments of the baseline minus those of the experiment that uses IASI over land) are shown in figure 11 for two levels (700hPa and 400hPa) averaged over the first month of the experimental period. The small magnitude of the changes may be partly related to the conservative thresholds applied to the IASI land data, resulting in radiances with large departures being excluded. However, the presence of other existing land observations in the analysis (satellite and conventional) may render large additional adjustments of the atmosphere unnecessary at the locations where the extra IASI data are being used. It is interesting to note that in the upper troposphere the RMS temperature increments are reduced over the central USA – an area that is densely observed with conventional data. The reduction in increments indicates that the assimilation of IASI over land has improved the analysis such that less adjustment is required.

Further evidence of an improved analysis is seen in the fit of the assimilation to other observations. The assimilation of additional IASI data over land improved the analysis fit to AMSU-A radiance data (figure 12 upper) and radiosonde temperature data (figure 12 lower). The reduction in the standard deviation is very small in these globally averaged statistics, but is a clear indication that the IASI land data are being used safely and add value to the analysis.

4.3 Changes to the forecast when IASI is used over land

Forecasts have been run from the baseline assimilation and the experimental system that uses IASI radiances over land. Zonally averaged RMS forecast error statistics (verified against each systems own analysis) are shown in figure 13 for vector wind and geopotential. Blue shading indicates the system that uses IASI over land has smaller forecast errors than the baseline while red shading indicates the opposite. Hatching shows where differences have been determined as statistically significant at the 90% level. From the predominance of blue shading it can be seen that the assimilation of IASI over land produces marginally better forecasts in most areas. The only exception is the geopotential forecasts at high southern latitudes over Antarctica, but these are not determined to be statistically significant.

5. Summary and suggestions for future activity

From the statistics of IASI window channel departures evaluated when the IASI pixel is homogeneous and free from cloud, we have gained some insight into the magnitude and variability of skin temperature information from the ECMWF NWP model. For the population of locations passing the

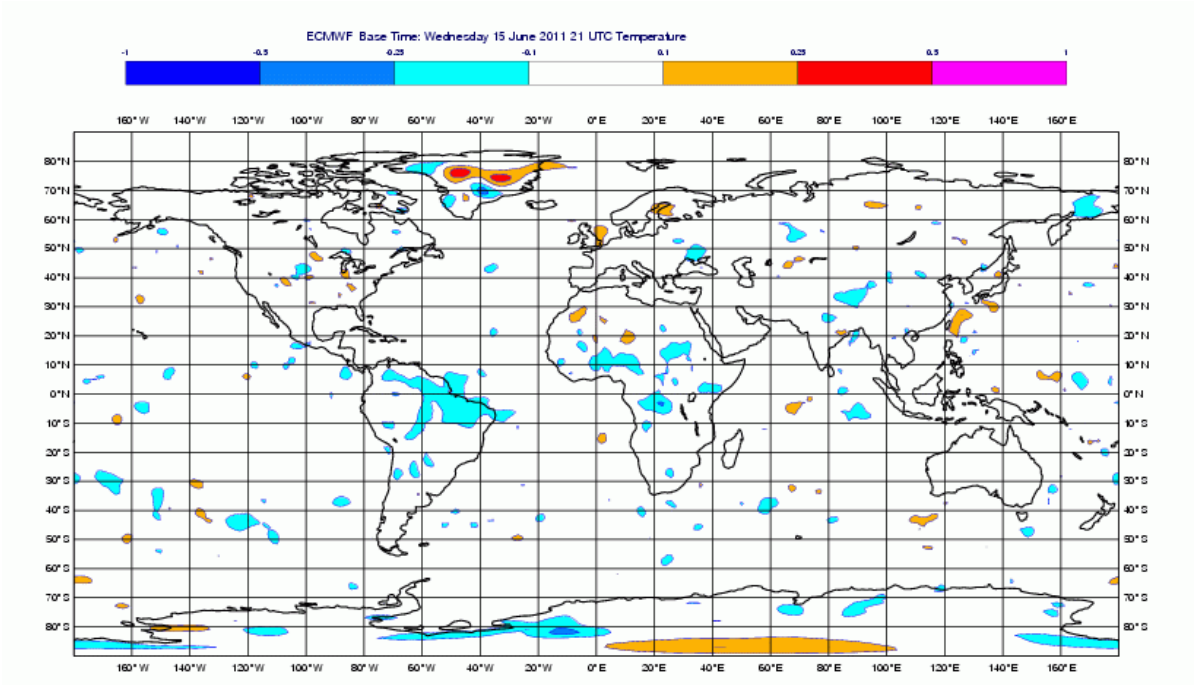

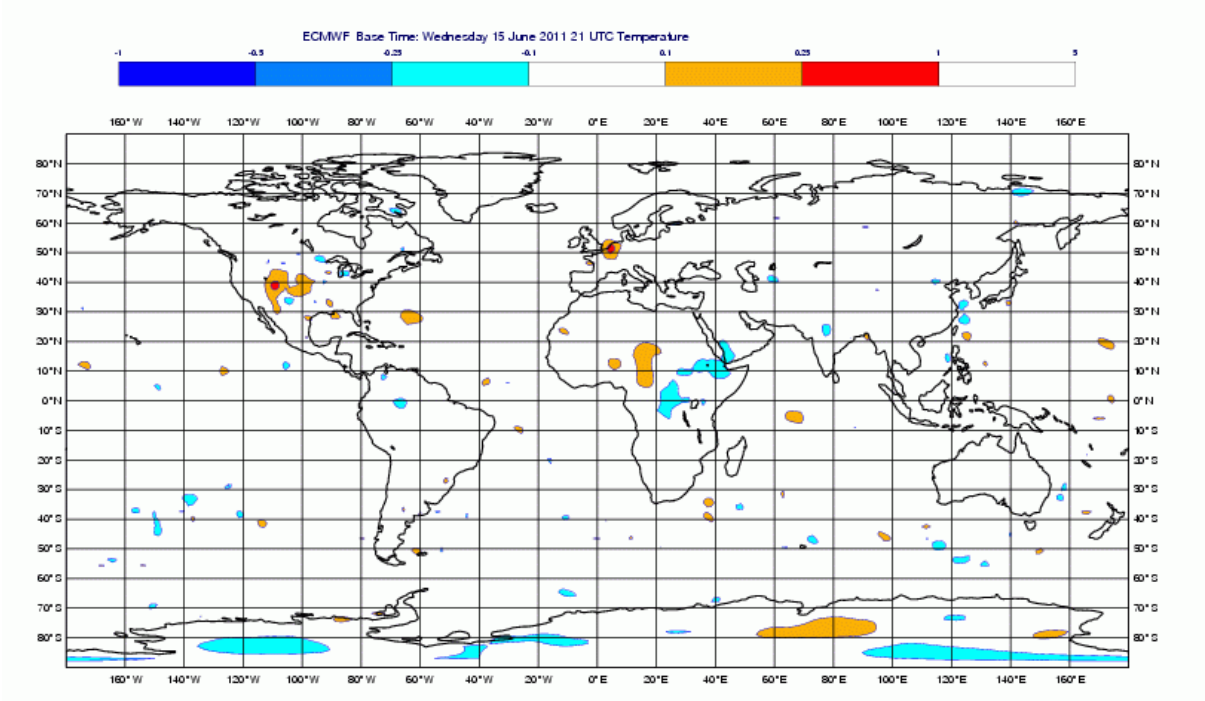

Figure 11 Root Mean Square temperature increment differences (baseline minus experiment) evaluated over the first month of the test period (June 2011) at 700hPa (upper panel) and 400hPa (lower panel)

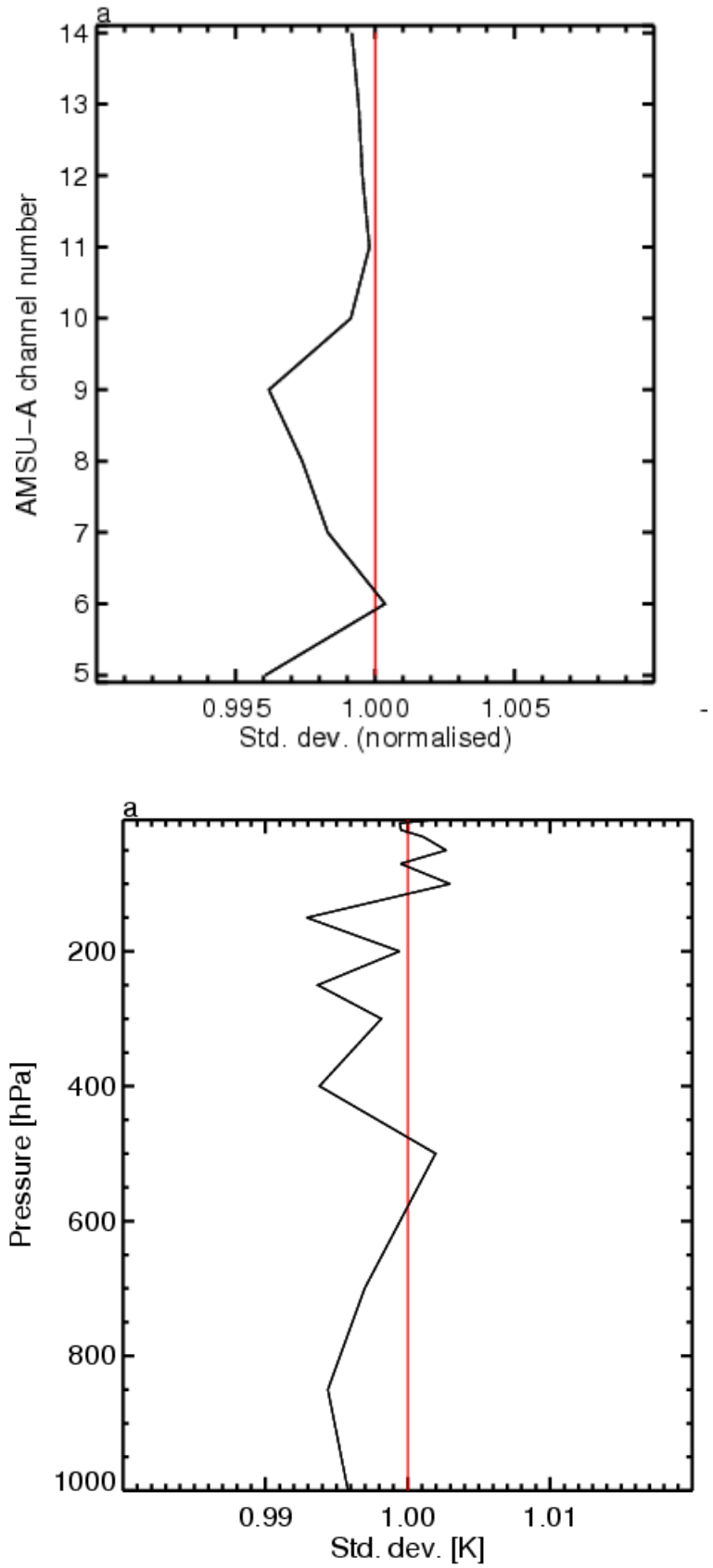

Figure 12 Standard deviation of the fit to AMSU radiances (upper panel) and TEMP temperature data (lower panel) for the June 2011 period. In both cases the reduction (improved fit) is expressed as a percentage of the baseline system fit to these data.

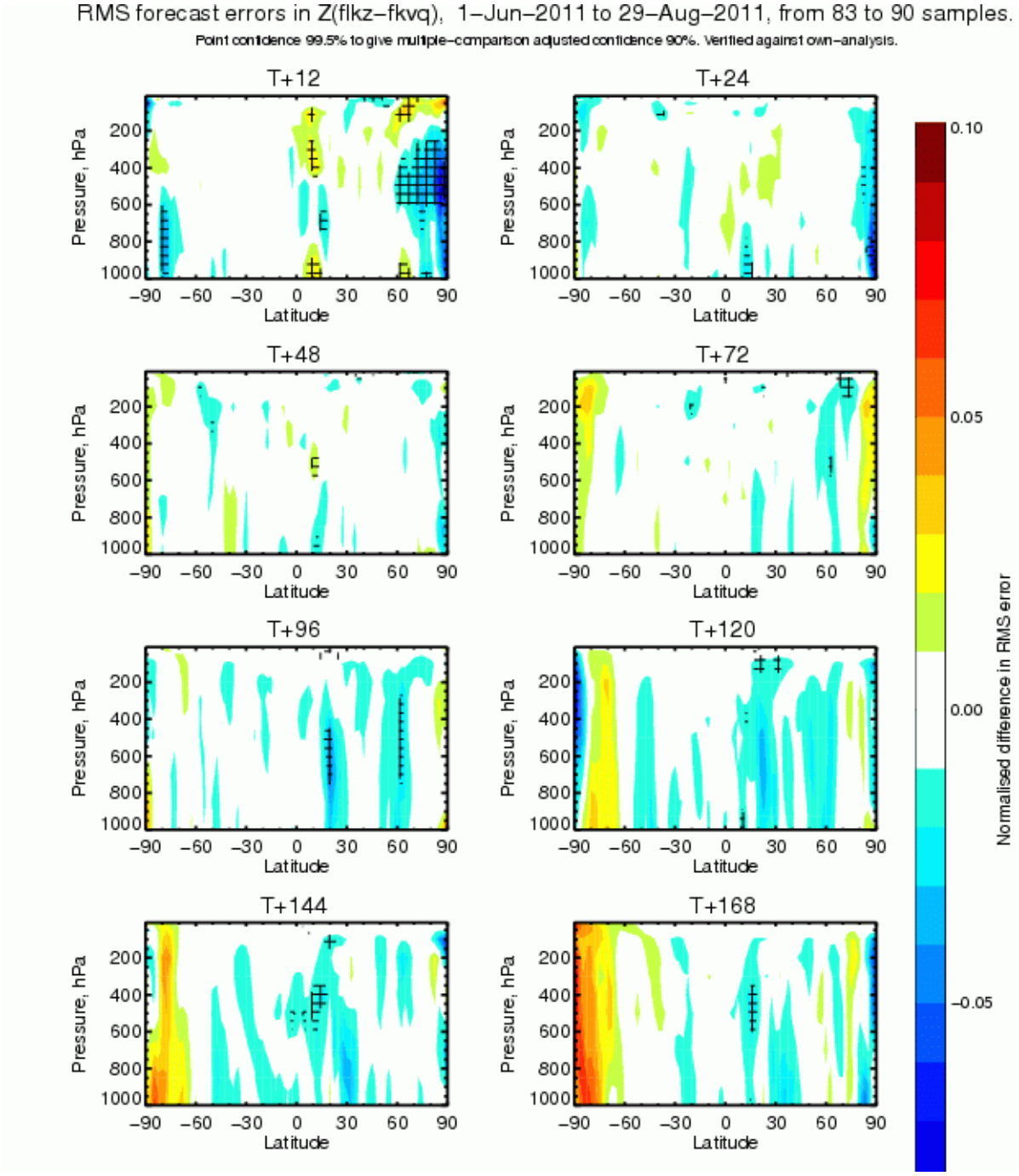

Figure 13 Percentage changes in RMS forecast error (experiment minus baseline) for geopotential height averaged over the full three month test period. Blue shading indicates where the experiment that uses IASI over land has reduced forecast errors. Red shading indicates the opposite. Hatched areas are determined statistically significant at the 90% level.

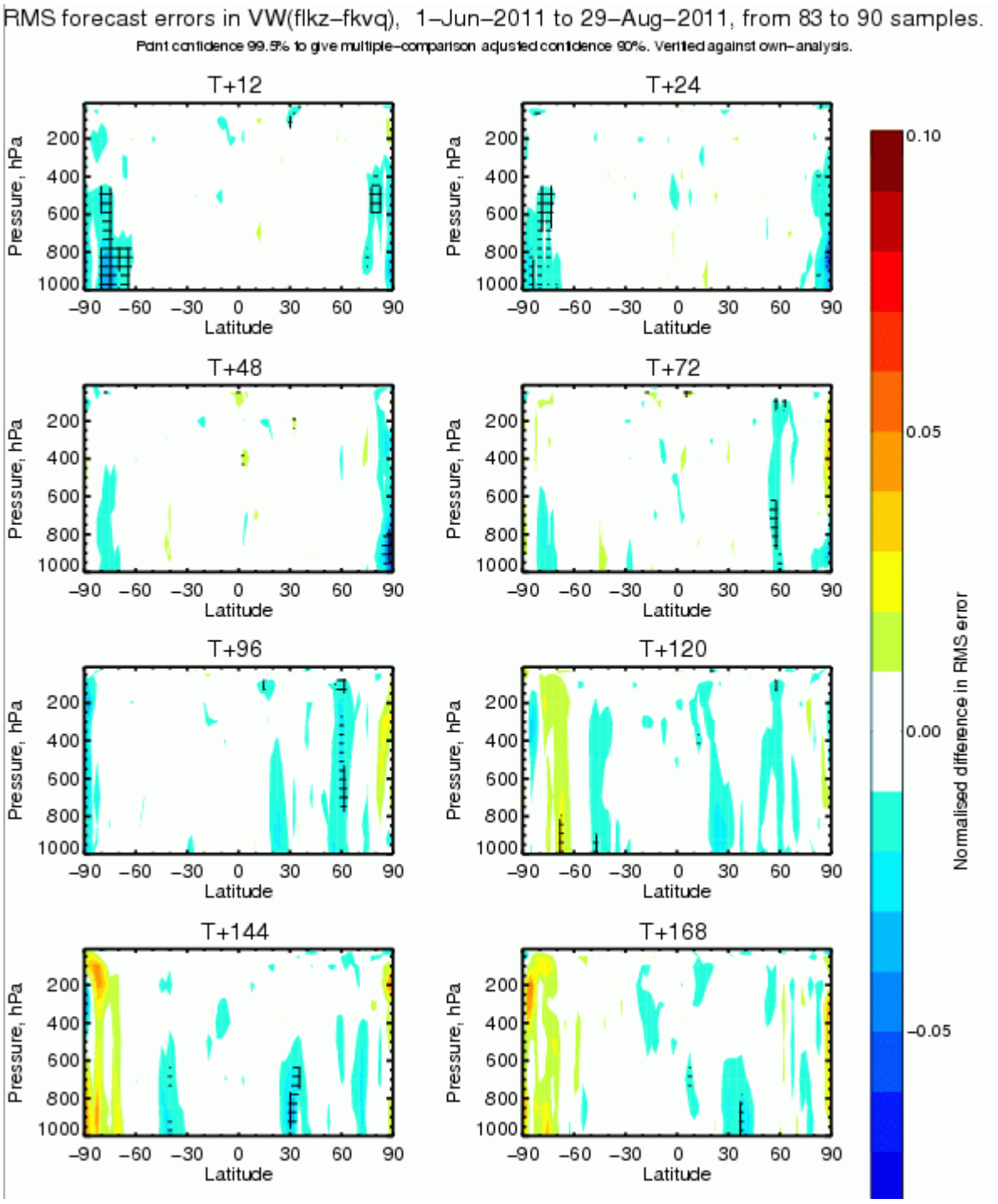

Figure 13 Percentage changes in RMS forecast error (experiment minus baseline) for vector wind averaged over the full three month test period. Blue shading indicates where the experiment that uses IASI over land has reduced forecast errors. Red shading indicates the opposite. Hatched areas are determined statistically significant at the 90% level.

rather stringent QC thresholds a reasonable global average figure for the standard deviation of the effective skin temperature error (i.e. one that incorporates uncertainty in the surface emissivity) is around 2.5K. Errors are larger and more variable over more complex terrain as indicated by the correlation with low values of Leaf Area Index (i.e. bare soil / desert). Densely vegetated land surfaces show much smaller skin temperature errors. However, it must be pointed out that these values are only applicable to the land surfaces observed by IASI (at its local passing time) and for the population that passes the strict quality control employed in this study. Satellites seeing different land surfaces, or even the same land surfaces at different times of day may be exposed to significantly different effective skin temperature errors.

In simulation, it has been shown that even the standard 366 IASI channel set contains a significant amount of information to estimate the effective surface skin temperature. With the assumptions made in this study regarding background errors and radiance observation errors, the skin temperature can be determined to better than 0.5K in dry conditions and around 1K in moist tropical conditions (where the surface is partially obscured by water vapour). Furthermore, the simulations also indicate that the surface skin temperature can be determined largely independently from the atmospheric parameters in the levels above the surface. This is important as it suggests that the IASI atmospheric information can be successfully exploited over land as long as the skin temperature is estimated simultaneously. In this context it was found that background errors for skin temperature should be overestimated if considerable uncertainty exists about their magnitude. Lastly, it was found that the offline simulations could mimic skin temperature adjustments in the full 4D-VAr system rather well. This suggests that the additional constraints of balance, model physics and other observations act only weakly on the skin temperature sink variable.

Real assimilation experiments have been performed using IASI radiances over land. The same channels that are used over sea are used over land, but a different approach to cloud detection has been employed. The homogeneity of AVHRR imger pixels inside the IASI field of view is considered a safer indicator of cloud contamination in mid-lower tropospheric channels than the algorithm used over ocean that relies on an accurate prior estimate of the surface emission. Results from the assimilation experiments show the skin temperature variable being adjusted as expected with only modest adjustments to the atmosphere above. However, the slightly improved fit to AMSU radiances and radiosonde observations suggest that the IASI data used over land do add value to the analysis. Furthermore, these improvements to the analysis have resulted in small, but statistically significant gains in forecast accuracy.

Some suggestions for future developments in this area are listed below:

Arguably one of the most serious limitations of the scheme tested here is that results in a rather limited geographical coverage. The land surfaces treated are those that can be determined cloud free from the AVHRR pixel test and – in its current form – cannot distinguish homogeneous clear cold surfaces from homogeneous cloud cover. Refinements of this test would allow the IASI data to be used over frozen high latitudes land surfaces in the winter allowing for a substantial gain in coverage.

The specification of background errors is limited to a simple global average value in this study, but there is no reason why this could not be made more sophisticated. Leaf area index is a good indicator of when we expect skin temperature errors to be larger and it could be used as a dynamic predictor for the assumed background error.

The IASI radiance information could also be enhanced by the inclusion of short-wave window channels. These have a significantly reduced sensitivity to water vapour (compared to the long-wave window channels) and could thus improve surface estimation in the tropics. However, these channels could only be used at night and place greater emphasis on the specification of variable surface emissivity.

Indeed no attempt has been made in this study to separate the uncertainty in skin temperature from that of the surface emissivity. This is not seen as a priority while the primary motivation to use IASI data over land is to improve the atmospheric analysis for NWP. For this purpose the only requirement is to separate the combined surface emission from the atmospheric signal in the IASI radiances and this is achieved with the effective surface sink variable. Efforts to supply more sophisticated emissivity information (e.g. from atlases) or to model (and estimate) emissivity explicitly may lead to a more physical estimate of surface skin temperature being obtained (that could possibly be used by the forecast model).

Acknowledgements

The authors would like to acknowledge the EUMETSAT NWP-SAF for funding this Visiting Scientist Mission to ECMWF and Naval Research Laboratory for releasing Ben Ruston. Many people at ECMWF contributed directly to the success of this study: Marco Matricardi for IASI Jacobians and error estimates, Elias Hólm for background errors and moisture variable transformation, Reima Eresmaa for providing alternate analysis error estimate for verification and validation, Alan Geer for verification of experiments and validation of radiometers, Anne Fouilloux for help with ODB interpretation and augmentation, Fernando Li with graphic generation and use of MetView, and Mohamed Dahoui with the examination of operational statistics. Also many fruitful discussions among the staff in the Satellite and Data Assimilation sections at ECMWF on interpretation and directions were extremely helpful and for their patience and extra guidance provided we'd like to thank: Niels Bormann, Bill Bell, Stephen English, and Yannick Tremolet.

ANNEX A The handling of T* for during outer-loops of 4D-Var

During the course of this study an error was discovered in the handling of the skin temperature sink variable between the outer loops of the 4D-Var system. During each inner loop the minimisation adjusted the variable and the end result should have been passed to initialise the minimisation of the next out loop. This was found to be done incorrectly, such that each outer loop was being initialised with the background value. The correction of this error was tested and found to have a small but positive impact upon the baseline system (that only uses radiance data over ocean) and was thus adopted for the purposes of this study.

References

Boussetta, S., Balsamo, G. Beljaars, A., Kral, T., and L. Jarlan, 2011: Impact of a satellite-derived Leaf Area Index monthly climatology in a global Numerical Weather Prediction model, *Int. J. Remote Sensing* (accepted), also available as *ECMWF Tech. Memo. 640*.

Gustafsson, N., Thorsteinsson, S., Stengel, M., and E. Hólm, 2011: Use of a nonlinear pseudo-relative humidity variable in a multivariate formulation of moisture analysis. *Q. J. R. Meteorol. Soc.*, **137**, pp.1004–1018.

Holm, E. and Andersson, E. and Beljaars, A. and Lopez, P. and Mahfouf, J-F. and Simmons, A.J. and Thepaut, J-N. Assimilation and Modelling of the Hydrological Cycle: ECMWF's Status and Plans September 2002

Matricardi, M., Chevallier, F., Kelly, G. and Thépaut, J.-N, 2004: An improved general fast radiative transfer model for the assimilation of radiance observations. *Q. J. R. Meteorol. Soc.*, **130**, pp.153–173.

Matricardi, M., 2009: Technical Note: An assessment of the accuracy of the RTTOV fast radiative transfer model using IASI data. *Atmos. Chem. Phys.*, **9**, pp. 6899-6913.

McNally, A. P., 2000: Estimates of short-range forecast-temperature error correlations and the implications for radiance-data assimilation. *Q. J. R. Meteorol. Soc.*, **126**, pp. 361-373.

McNally, A. P. and P. D. Watts, 2003: A cloud detection algorithm for high spectral resolution infrared sounders. *Q. J. R. Meteorol. Soc.*, **129**, pp. 3411-3423.

McNally, A. P., 2009: The direct assimilation of cloud-affected satellite infrared radiances in the ECMWF 4D-Var. *Q. J. R. Meteorol. Soc.*, **135**, pp. 1214-1229.